

Manuscript Number:

Title: Pin-on-disc study of a friction material dry sliding against HVOF coated discs at room temperature and 300°C

Article Type: Full Length Article

Keywords: Dry sliding; HVOF coatings; Friction material; High-temperature wear tests

Corresponding Author: Professor Giovanni Straffelini, Full professor

Corresponding Author's Institution: Università di Trento

First Author: Giovanni Straffelini, Full professor

Order of Authors: Giovanni Straffelini, Full professor; Matteo Federici, Ph.D. student; Cinzia Menapace, Professor ; Alessandro Moscatelli, eng.; Stefano Gialanella, Professor

Abstract: The sliding behavior of a commercial semi-metallic friction material against an uncoated cast iron disc and HVOF coated discs at room temperature and at 300°C has been investigated. At RT, a quite long initial stage was observed, required to form a compact friction layer and to achieve a constant friction coefficient. At 300°C, steady-state conditions are attained almost from the beginning of the test. The wear rates of the friction materials are mild at room temperature and close to severe at 300°C because of the thermal softening of the friction material. The wear rates of the coated discs are always negligible, since the contact temperature is not sufficiently high to induce a softening or an oxidative damage of the coatings.

Suggested Reviewers: Werner Osterle
Head, BAM Bundesanstalt Mat Forsch & Prufung, BAM Bundesanstalt Mat
Forsch & Prufung
werner.oesterle@ban.de
Recognized expert in braking systems as well as in tribology in general.

Peter Filip Professor
Center for Advanced Friction Studies, Carbondale (US)
filip@siu.edu
Recognized expert in the friction and wear of braking systems.

Maria D. Salvador Professor
Instituto de Tecnologia de Materiales Universidad Politecnica de
Valencia, Spai, Universidad Politecnica de Valencia, Spain
dsalva@mc.upv.es
Expert in thermal coatings and their characterization (including wear
behavior).

To the Editor-in-Chief of
Tribology International
Dr. Michel Fillon

Dear Dr. Fillon,

I am submitting for the publication in this Journal, also on behalf of the other co-Authors, the paper:

Pin-on-disc study of a friction material dry sliding against HVOF coated discs at room temperature and 300°C

By M. Federici et al.

The work was carried out within an european project under the Horizon 2020 programme. The project is aimed at developing systems to reduce the pollution induced by the wear of vehicle braking systems.

The present investigation starts from the observation that wear of the disc also plays an important role. We therefore proposed to coat the discs using commercial HVOF coatings.

This is a preliminary investigation based on a Pin-on-Disc test procedure. The main aim was to understand the wear mechanisms, including the formation of the friction layer that plays an important role in friction and wear of these systems. The tests were carried out at room temperature and also at 300°C to understand the possible role of severe braking conditions.

thank you very much for you attention!

Giovanni Straffelini

We look forward to your reply!

Kind Regards.

Giovanni Straffelini and co-Authors.

Statement of Originality

Dear Editor

The present research has been carried out within the LOWBRASYS project, which is funded by the European Union's Horizon 2020 programme, and is aimed at developing new friction materials and discs with reduced environmental impact.

Most experimental investigations on the reduction of the wear in braking systems have been especially focused on the optimization of the friction materials, by selecting suitable ingredients and relevant concentrations. The present research is focused instead on reducing the disc wear by thermal spray (two commercial coatings sprayed by HVOF were selected) that is known to reduce sliding wear in tribological system.

The role of the coatings have been investigated and the results have been explained making specific reference to the acting wear mechanisms and the corresponding characteristics of the friction layer [building up between the pin-disc mating surface during the tests](#). Special emphasis has been reserved to the characterization of the friction layer that is known to play an important role in the tribological system under study. Tests were carried out at room temperature as well as at 300°C to understand the system response in case of severe sliding conditions.

The experimental set up has not been designed with the intention the real brake system action, for which specific equipment, like dyno tests, are available and will possibly used in the future to optimize all the engineering requirements of a real braking system.

Best regards
Prof. Giovanni Straffelini
University of Trento

Research Highlights

- Wear of coated discs is always negligible.
- Wear of pins is mild at RT and increases very much at 300°C.
- At 300°C, the formation of a wide and thick friction layer is observed.
- At 300°C, steady-state conditions for friction and wear were reached soon.

Pin-on-disc study of a friction material dry sliding against HVOF coated discs at room temperature and 300°C

Matteo Federici^a, Cinzia Menapace^a, Alessandro Moscatelli^b, Stefano Gialanella^a, Giovanni Straffelini^{a*}

^a Dept. of Industrial Engineering, University of Trento, Via Sommarive 9, Povo, Trento, Italy

^b Flame Spray, via Leonardo da Vinci 1, Roncello, (MB), Italy

* Corresponding Author

Abstract

The tribological behavior of a commercial semi-metallic friction materials dry sliding against an uncoated cast iron disc and HVOF coated discs at room temperature and at 300°C has been investigated. Two types of coatings were investigated, based on Cr₃C₂-NiCr and WC-CoCr systems. The tests were carried out using a pin-on-disc apparatus. The characteristics of the friction layer that forms on the worn surfaces of the friction material (the pin) and on the counterface disc were analyzed and correlated with the friction and wear behavior of the couplings. At room temperature, a quite long initial stage was observed, required to form a compact friction layer and to achieve a constant average friction coefficient. At 300°C, steady-state conditions are attained almost from the beginning of the test. The wear rates of the friction materials are mild at room temperature and close to severe at 300°C because of the thermal softening of the friction material. The wear rates of the coated discs are always negligible, since the contact temperature is not sufficiently high to induce a softening or an oxidative damage of the coatings. Although referring to rather simplified testing conditions, the results obtained in this study provide useful indications on the possibility of using HVOF coatings in braking systems to reduce not only their wear but also, most importantly, the release of particulate matter in the environment.

Key words:

Dry sliding; HVOF coatings; Friction material; High-temperature wear tests; Braking materials

1. Introduction

A significant contribution to the emission of particulate matter (PM) in the urban environment is to be ascribed to the formation of wear fragments from braking systems of road vehicles [1-3]. One of the major findings of these studies was the comparable contribution of pads and cast iron discs to the PM emissions [4]. Starting from this experimental observation and in order to reduce this source of emission, i.e., brakes, with particular regard to the wear of the discs, thermal spray coatings based on $\text{Cr}_3\text{C}_2\text{-NiCr}$ and WC-CoCr systems, deposited by the high-velocity-oxygen-fuel (HVOF) process, have been recently proposed and have obtained very promising results already [5].

By means of the HVOF technique, cermet coatings with excellent dry sliding properties can be obtained starting from relevant powders. Typical HVOF coatings show a hardness within the range of 900-1200 HV, depending on the type of carbides and metal matrix. The elevated velocities reached by the sprayed particles during the process (up to 500 m/s) lead to the deposition of coatings with low residual porosity and, consequently, improved wear resistance [5-12]. Room temperature wear properties of these coatings, sliding against a steel or a ceramic counterpart, were studied by several authors [13-15] and all of these investigations detected specific wear coefficients in the range 10^{-16} - 10^{-14} m^2/N , that are typical of a mild wear regime. Wang et al. [16] have identified the room temperature wear mechanisms of these coating systems as mostly due to delamination, fracture of carbides, metallic phase cracking with the subsequent disruption of the carbide-binder interfaces, microcutting, and extrusion of the binder phase. Bolelli et al. [17] extended the study of the wear mechanisms of the HVOF-cermet coatings to the high temperature regime. During their tests, the wear rate of the WC-CoCr coatings, sliding against an alumina counterpart, increased by two order of magnitude (from 10^{-16} to 10^{-14} m^2/N) by increasing the testing temperature from room temperature to 750°C . They associated this increase in the wear rate to the different wear mechanisms activated at different temperatures. At 400°C the matrix of the WC-CoCr coating softened, leading to a first increase in the wear rate. At 600°C a thin oxide layer, that was able to withstand a remarkable strain, was formed on the surfaces of the two mating bodies. It acted as solid lubricant and prevented the severe wear of the two bodies. At 750°C the oxide layer became thicker and more brittle, leading to the severe wear of the coating [17]. Zhang et al. [10] compared the high temperature wear performances of WC-10Co-4Cr and $\text{Cr}_3\text{C}_2\text{-25NiCr}$ HVOF coatings; according to their study the $\text{Cr}_3\text{C}_2\text{-25NiCr}$ coating showed a higher wear resistance than the WC-10Co-4Cr one.

Most of the sliding tests carried out so far on HVOF cermet coatings, use steels or ceramic materials as counterface. To the Authors' knowledge, just a few works have been carried out so far using a braking friction material as a counterface in wear experiments [5,18]. The typical average surface roughness (R_a) of the coatings in the as-sprayed conditions is around $5\ \mu\text{m}$ [5,6,18]. In a previous investigation, the effects of roughness on the friction and wear behavior of a WC-CoCr coating dry sliding against a commercial low-metallic friction material have been investigated using a pin-on-disc apparatus [5]. The wear rate of the friction material (the pin) was found to increase with the coating roughness and to become very high when R_a was in excess of $1\ \mu\text{m}$. In all cases, the wear of the coating was negligible.

The friction and wear behavior of braking friction materials is controlled by the characteristics of the friction layer that forms at the interface of the mating bodies [19,20]. The performances are quite sensitive to the contact temperature. When it is above 250°C approximately, the wear rate of the friction materials starts to increase and wear may become severe, because of the thermal softening of the polymeric binders [21-23]. In the present investigation, the friction and wear behavior, at both room and at 300°C , of the two differently-coated brake discs sliding against a commercial low metallic friction material has been investigated. The experimental tests were performed by means of a pin-on-disc (PoD) apparatus and the average surface roughness of the HVOF coated discs was decreased to values of around $1\ \mu\text{m}$. The aim of the work was to achieve a better insight on the behavior of the two coatings sliding against a brake friction material, with special emphasis on the role of the contact temperature on the characteristics of the friction layer and the relevant friction and wear behavior of the coupling. It is expected to obtain useful information to be used for subsequent dynamometric tests aimed at understanding the sliding behavior of a real brake pads and related environmental emissions [24].

2. Materials and experimental procedures

The coatings were deposited by the HVOF technique onto pearlitic cast iron discs with a diameter of 63 mm. Two types of commercial powders were used, whose nominal compositions are listed in Table 1. The grains of the powder used for Coating A are made of WC particles embedded in a Co-Cr matrix. The powder for Coating B features Cr_3C_2 particles embedded in a metallic matrix made of a Ni-Cr alloy. The coatings were produced in standard conditions, with a spraying distance of 380 mm, a kerosene flux of 25 L/h and oxygen flux of 1000 L/min [6-12]. A coating thickness of about 70 μm was obtained. Cross sections of the coatings in the as-sprayed condition are shown in Figure 1. The surface roughness was relatively high, with an average roughness above 5 μm . Following previous results [5], the coated discs were polished with a SiC paper (220 grit), thus reducing R_a to about 1 μm . Figure 1 shows that the coatings are characterized by a relatively low porosity and by the absence of observable cracks. Table 1 lists the microhardness of the coatings, obtained on the cross sections using a Vickers indenter and a load of 300 g.

Table 1: main characteristics of the coatings A and B.

Coating	Starting powder composition (wt.%)	Starting powder particle size	HV0.3
A	86% WC / 10% Co / 4% Cr	10-25 μm	1130
B	75% Cr_3C_2 / 25% NiCr	10-45 μm	920

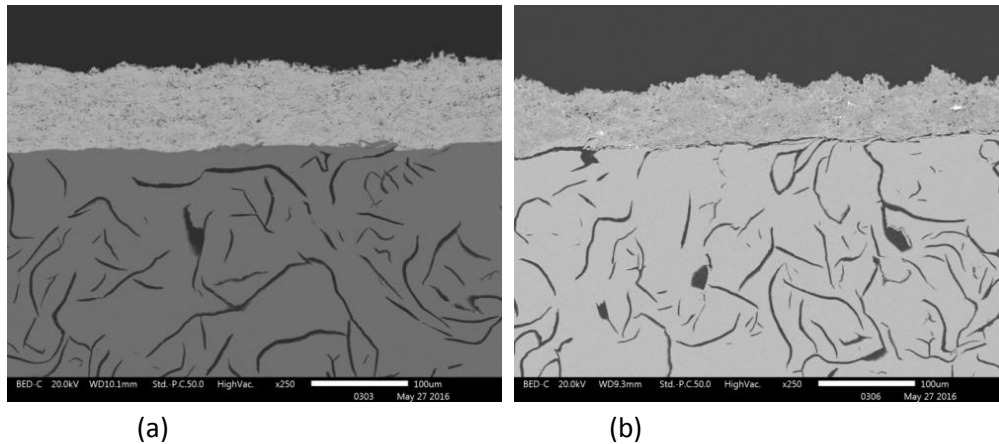


Fig.1. SEM micrographs showing the cross section of the as-sprayed coatings A (a) and B (b).

The XRD analysis on coated discs, obtained using $\text{Cu-K}\alpha$ radiation, are shown in Fig. 2. In coating A the presence of W_2C in addition to WC has been detected. The presence of W_2C is usually attributed to some decarburization occurring during the HVOF process [10,25-27]. This phenomenon depends on the deposition conditions, particularly the high temperature, an oxidizing atmosphere and high cooling rates, so that the sprayed material is subjected to complex physical and chemical transformations [25-28]. The amount of WC and W_2C measured by XRD and evaluated using the Rietveld method [29], were 46 wt.% and 54 wt.%, respectively. The CoCr matrix turned out to be amorphous, in agreement with literature data on similar coating systems [30]. The phases identified by XRD in coating B were Cr_3C_2 (45 wt.%) and Ni (55 wt.%).

The friction material adopted for the present investigation was a commercial low-metallic friction material, comprising different ingredients embedded in a polymeric matrix. Table 2 lists the chemical composition of the material, as obtained by a full field EDXS analysis. The microstructure of the material with the identification of some of the main ingredients is shown in Figure 3. It can be observed that the majority elements are Fe, Cu and C. Fe and Cu are present in form of fibers and particles of different size. It can be further noted that C, added in different forms, i.e., graphite, coke, behaves as solid lubricant and it is also the main constituent of the binder, which is a phenolic resin.

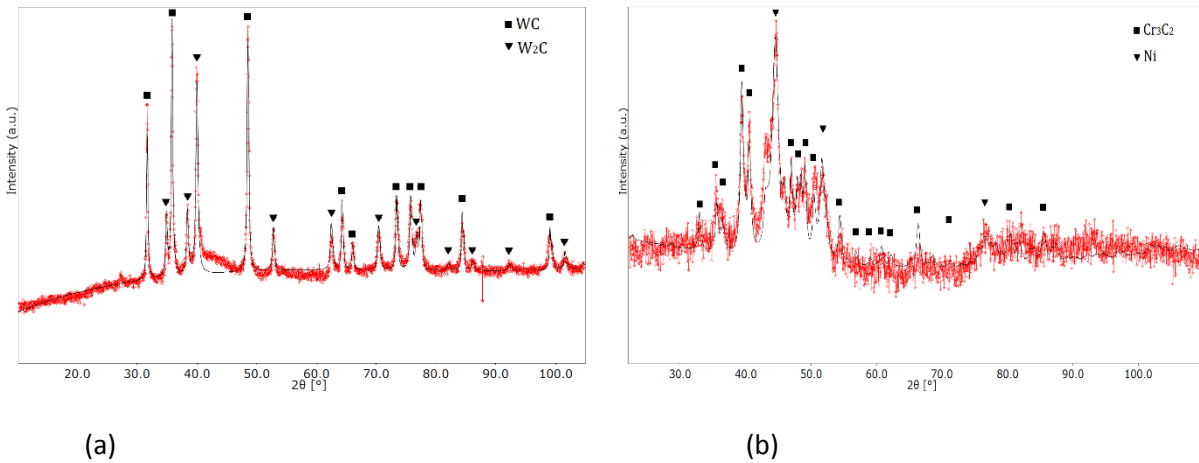


Fig.2. XRD spectra of coatings A (a) and B (b).

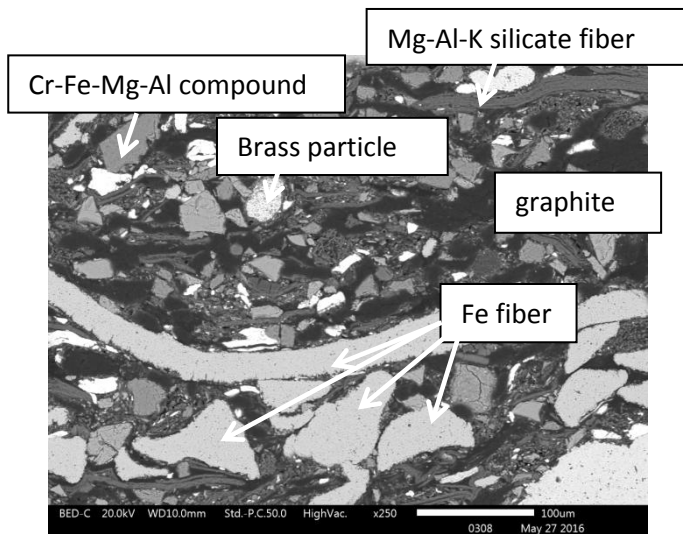


Fig.3. SEM micrograph of the surface of the friction material, with the indication of some of the main components

Table 2: Composition of the friction material, as evaluated from EDXS analyses.

Element	Wt.%	Element	Wt.%
Fe	23.3	Mg	4.9
C	16.6	Al	7.2
Cu	15.6	Si	2.3
Sn	3.7	Cr	2.3
Zn	7.7	K	0.7
Ca	0.5	S	2

The thermal behavior of the friction material was investigated with a thermogravimetric instrument (TGA). The continuous heating TGA curve of Fig.4 (carried out in air) shows a weight loss of about 5% which starts at approximately 330°C, with a maximum decomposition rate around 407°C, confirmed by the differential DTG curve. The weight loss is due to the decomposition of the phenolic resin, and the oxidation of carbon, leading to the formation of H₂O and CO₂. The temperature of the resin decomposition is in agreement with literature data, reporting on a thermal degradation of the organic components of the friction material over a temperature range from 200 to 450°C [25-28]. As known, the resin degradation is responsible for tribological behavior of the friction materials at increasing contact temperature [25]. Although not strictly relevant to the friction behavior, it is worth noticing that the thermogravimetric curve continues to record a weight decrease, even above 450 °C. A stable level is achieved above 600°C (see label at 613 °C in figure 4). This further weight reduction can be ascribed to a progressive release of the gaseous products coming from the decomposition of the polymeric resin with an additional contribution from the dehydration reaction involving the silicate clay based components of the friction material.

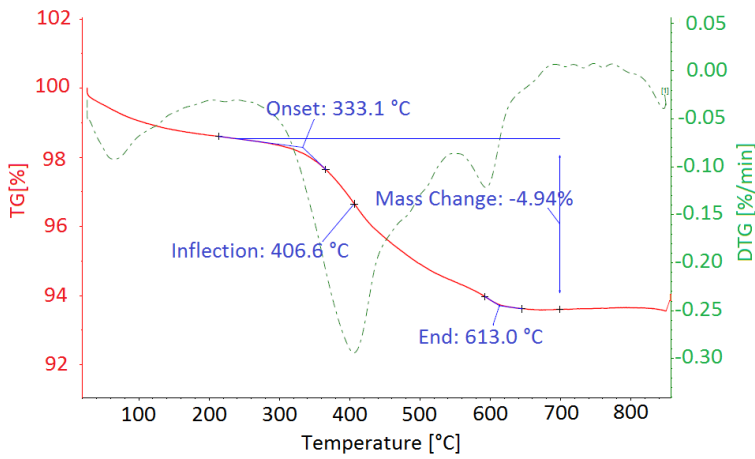


Fig.4. TG and DTG curves of friction material.

Dry sliding tests were carried out using a PoD testing instrument. The pins (with a diameter of 6 mm) were machined from commercial brake pads. On the basis of a previous study [21], the tests were carried out at room temperature and at 300°C at a sliding velocity of 1.57 m/s for 50 min after a running in step of 10 min. The tests at 300°C were carried out using a test arrangement described in Ref. [25]. A heating coil was used to heat the disc temperature at 300°C. A closed loop feedback system was used to maintain the temperature constant through an infrared temperature sensor. The nominal contact pressure applied was 1 MPa. Pin wear was measured by evaluating the weight loss using an analytical balance with a precision of 10⁻⁴ g. Wear volumes were determined by dividing the weight loss by the density of the pin (2.9 g/cm³). The specific wear coefficient, K_a (m²/N), was calculated using the following expression:

$$K_a = V / (s * F_N)$$

where V is the measured wear volume, s is the sliding distance and F_N is the applied load. The wear of the disc was evaluated by a profilometer analysis.

During the test the friction coefficient was continuously recorded. The evolution of the pin temperature was also monitored through two thermocouples inserted in the pin at a distance of 4 and 6 mm from the contact surface. Worn pins and discs were examined through optical and scanning electron microscopes.

A scanning electron microscope (SEM), used to characterize the friction material and to examine the surface morphology and composition of the worn pins and counterface discs, was equipped with an energy dispersive X-ray spectroscopy (EDXS) system.

3. Results

3.1 Friction and wear behavior at room temperature

Fig.5a shows the evolution of the friction coefficient during the wear test using uncoated disc. It exhibits an increasing trend with time lasting for 40 minutes approx. (stage S1). Then the curve reaches quite a constant value (steady state, stage S2). The average values of the friction coefficients for the initial and steady state stages (S1 and S2) are listed in Table 3. In Fig.5b the two pin temperatures measured during the same test as in fig. 5a are shown. In both cases, the temperature continuously increases with time showing that thermal equilibrium was not reached before the end of the tests. In Table 3, the pin temperatures recorded at the end of the tests are reported.

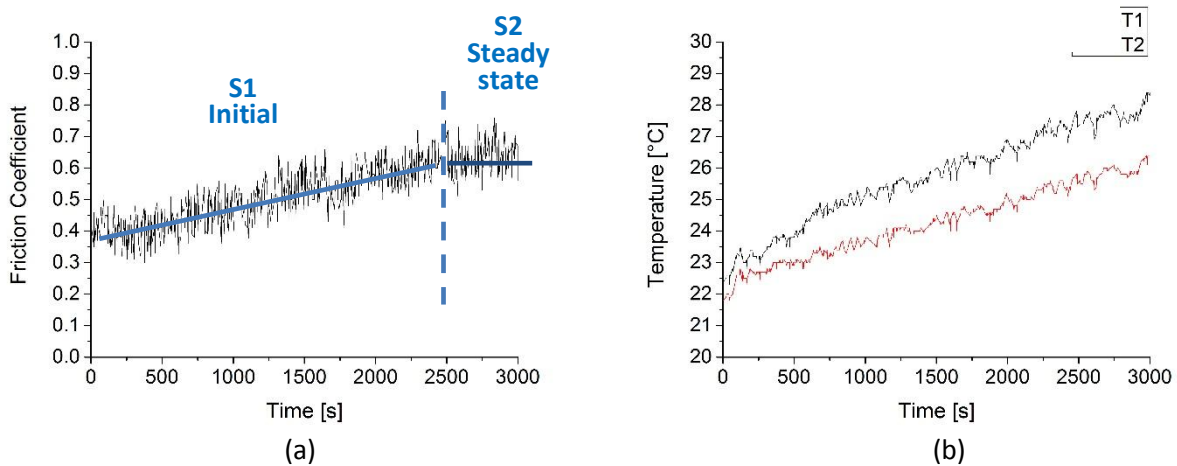


Fig.5. Evolution of the friction coefficient μ as a function of the wear test time (a) and contact temperature of pin measured by thermocouple at 4 mm (T1) and 6 mm (T2) from the disc surface during the test against the uncoated disc at room temperature (b).

Table 3

Friction and wear test results of friction material against uncoated and coated discs at room temperature.

	μ_i	μ_{ss}	T1 (°C)	T2 (°C)	Pin wear K_a (m^2/N)	Disc wear K_a (m^2/N)
Uncoated disc	0.4	0.63	28.3	26.8	$5.89 \cdot 10^{-14}$	$2.89 \cdot 10^{-14}$
Coating A	0.3	0.66	28.6	27.8	$1.26 \cdot 10^{-14}$	-
Coating B	0.43	0.59	28.2	26.4	$9.96 \cdot 10^{-15}$	-

Fig.6 shows the friction evolution in case of the two coated discs. The trends are very similar to those encountered in case of the uncoated disc, and relevant data are still included in Table 3. One difference concerns the duration of the first stage, that is shorter for coating B (25 minutes). The temperature records are not reported since they are very similar to those shown in Figure 5b.

In Table 3 includes also the results for the pin and disc wear. The disc wear was evaluated from the profilometer profiles shown in Figure 7. For both the coated discs no wear tracks were detected, indicating a very good wear resistance of these discs.

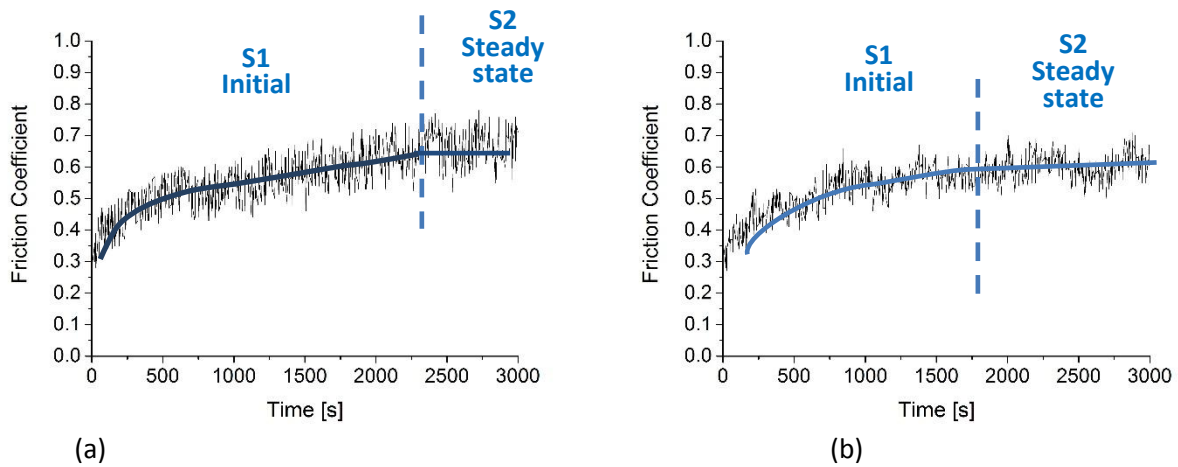


Fig.6. Evolution of the friction coefficient μ during wear tests carried out at room temperature. (a) results for the A (a) and B (b) coated disc.

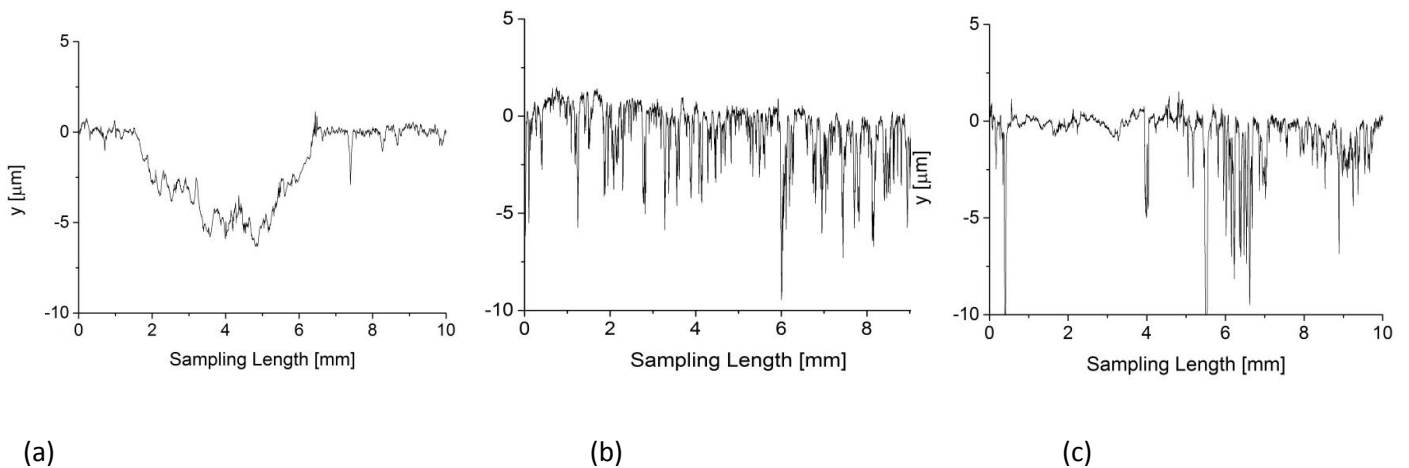


Fig.7. Wear track profile present on the disc surface after room temperature PoD tests. (a) Uncoated disc; (b) Coating A; (c) Coating B.

3.2 Friction and wear behavior at 300°C

During the PoD tests at 300°C, an almost constant evolution of the friction coefficient with time was recorded for the uncoated disc, as shown by Fig.8a. Figure 8b shows the pin temperatures evolution. They increase from about 70°C up to a maximum of 125°C at the end of the test. However, also in this case the thermal equilibrium does not seem to be reached. The results of the tests are reported in Table 4, where also the wear data are included. Please note that we were not able to measure the wear of the uncoated disc because of the transfer of debris from the friction material that counterbalanced any disc wear.

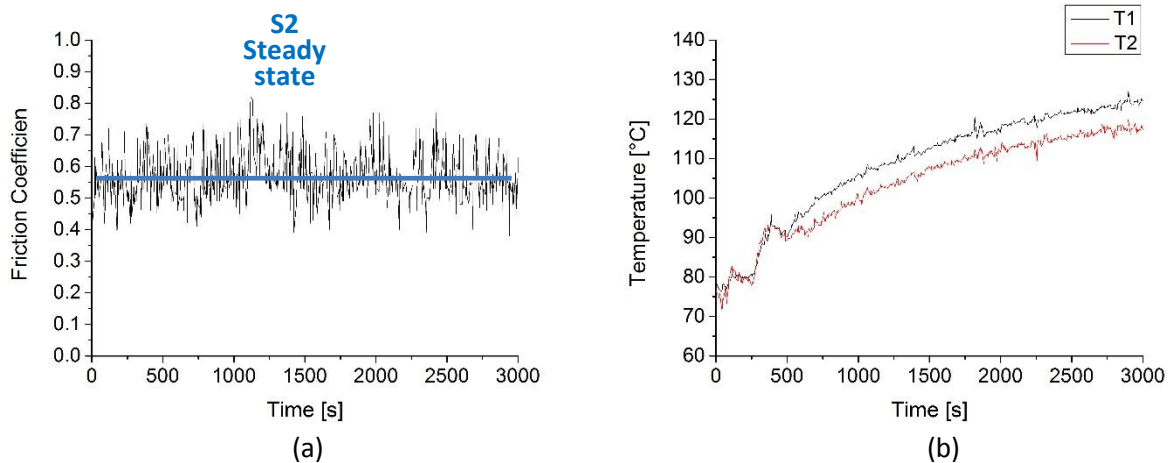
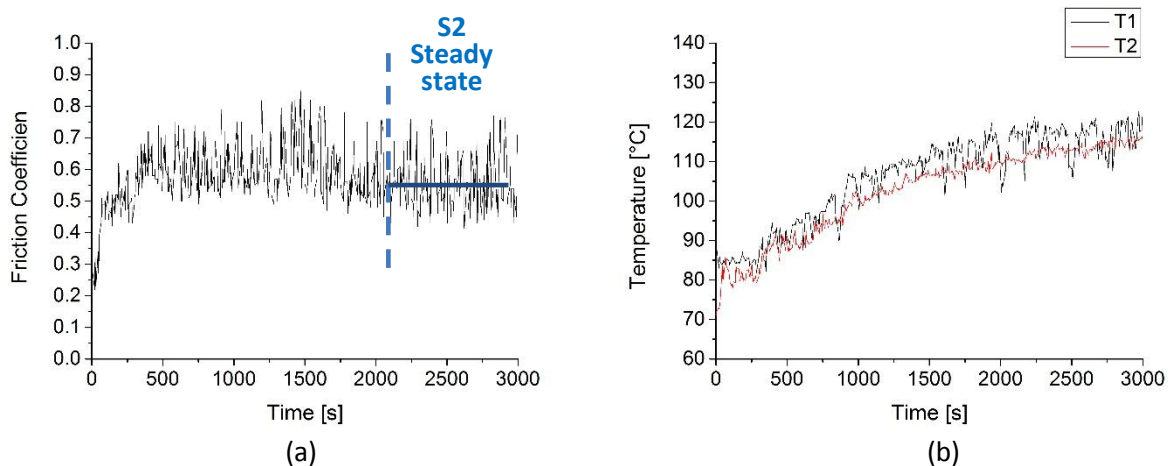


Fig. 8. Evolution of the friction coefficient μ (a) and of the pin temperature (b), during wear test against conducted with the uncoated disc at 300°C.

Figure 9 shows the evolutions of the friction coefficient and pin temperatures for the coated discs. In case of coating A, the friction coefficient, initially increased to approximately 0.64 then started decreasing reaching a value around 0.52 before the end of the test. In case of coating B, the running-in stage seems to be very short, and then a constant friction coefficient was reached soon (within 250 s).

Table 4
Friction and wear test results of friction material against uncoated disc at 300°C.

	μ_{ss}	T1 (°C)	T2 (°C)	Pin wear K_a (m^2/N)
Uncoated disc	0.57	124.2	117.5	$6.01 \cdot 10^{-14}$
Coating A	0.55	118	115	$6.67 \cdot 10^{-14}$
Coating B	0.46	115.2	110.6	$8.01 \cdot 10^{-14}$



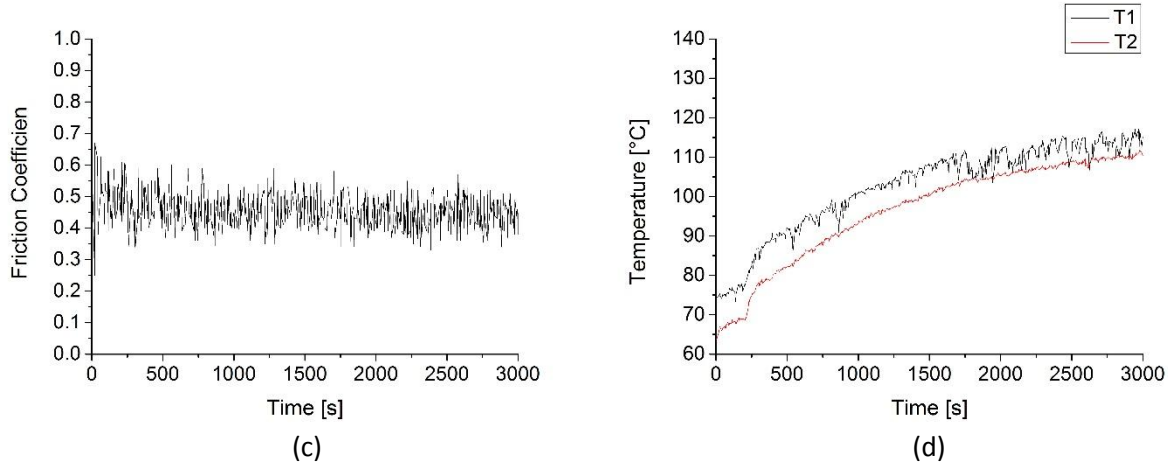


Fig.9. Evolution of the friction coefficient and of the pin temperature during PoD tests conducted on the two coating systems considered in the present study: Coating A: (a), (b); coating B: (c), (d).

3.3 Characterization of worn surfaces

Figures 10 and 11 show the planar and cross sectional views of the worn pins at the end of the tests carried out at room temperature. The friction layer building up on the worn surfaces is made of the so-called primary and secondary plateaus. The primary plateaus are typically made of the hardest ingredients of the friction material, such as the iron fibers or large ceramic particles [19,20,31]. The secondary plateaus are made by more or less densely compacted wear fragments, that accumulate against the primary plateaus. In the case of B coating, the secondary plateaus seem to be well compacted and close to the primary plateaus, as usually observed. For the uncoated and A-coated discs, the secondary plateaus partially cover the underlying primary plateaus: this would indicate that wear debris are much finer and not yet fully compacted. The cross sectional views of these specimens indicate that the thickness of the friction layers is relatively small, well below 10 μm in all cases.

The results of the EDXS analyses, carried out on the secondary plateaus on the worn pins are listed in Table 5 (each data point is the average of at least 4 measurements). They revealed, in case of uncoated disc, that the secondary plateaus are mainly constituted of iron, and then most probably by Fe oxides, in agreement with the results of former investigations [19,20,31]. In the case of coatings A and B, the friction layers contain all the principal constituents of the friction material together with elements coming from the counterface coating, i.e. W and Co in case of A and Cr and Ni in case of B (even if some Cr is present also in the friction material as reported in Table 2), most probably in the form of very small particles as reported in the literature [32,33].

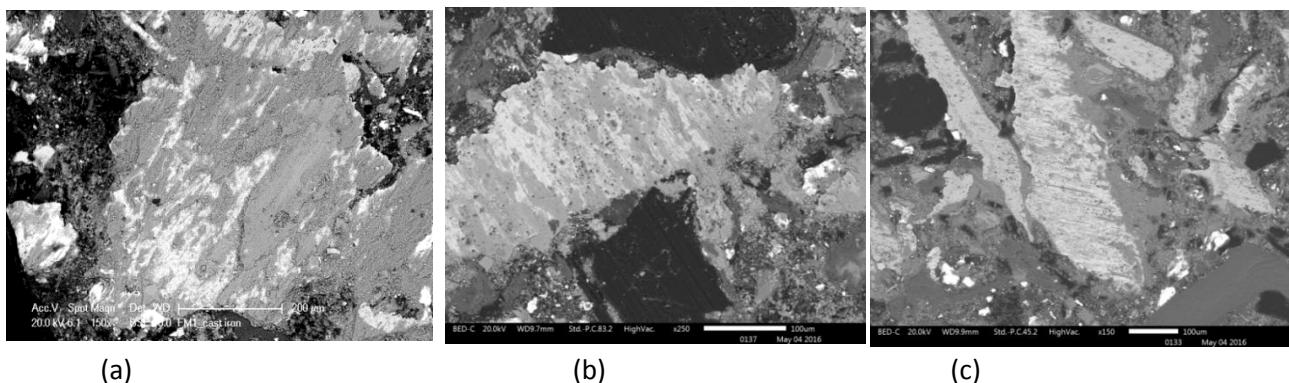
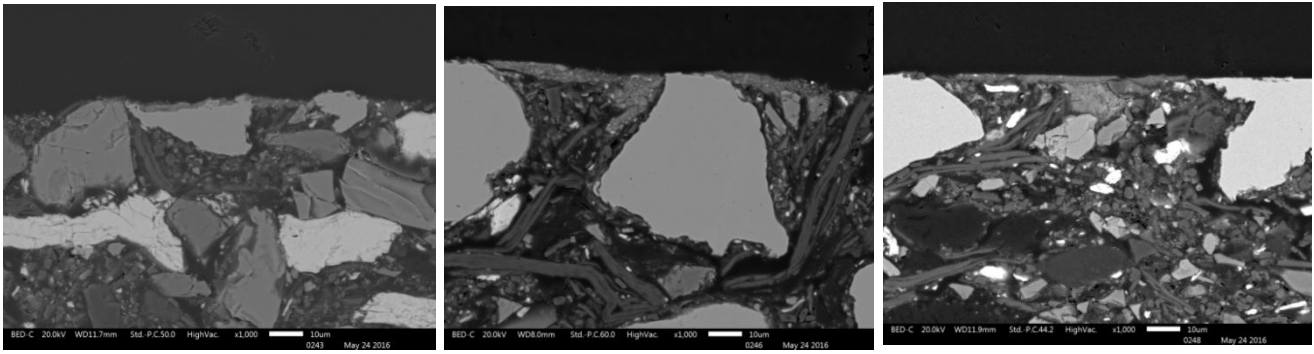


Fig.10. SEM micrographs of the planar views of friction materials PoD tested at room temperature, against uncoated (a), A-coated (b) and B-coated (c) discs.



(a)

(b)

(c)

Fig.11. Cross sectional SEM images of the worn surface of the friction materials PoD tested at room temperature against uncoated (a), A-coated (b) and B-coated (c) discs.

Table 5. Composition (obtained by EDXS analysis) of the secondary plateaus on the worn pins.

Uncoated disc			A			B		
Element	RT	300°C	element	RT	300°C	element	RT	300°C
Fe	79.9	46.1	Fe	34.6	34.3	Fe	10.3	25.7
Cu	9.1	26.2	Cu	22.5	17.7	Cu	5.4	5.0
Sn	1.6	5.3	Sn	4.2	6.0	Sn	-	6.4
O	3.9	3.7	O	4.1	3.3	O	4.9	7.5
Si	3.0	4.0	Si	1.1	1.7	Si	1.3	4.3
Al	0.6	9.2	Al	3.5	4.2	Al	11.1	6.0
Mg	1.1	3.0	Mg	1.9	2.5	Mg	-	4.9
Cr	0.8	2.5	Cr	2.7	11.4	Cr	44.2	26.8
			S	2.5	2.7	S	2.8	-
			Zn	4.7	7.2	Zn	6.3	6.0
			Co	1.5	0.3	Ni	13.7	6.7
			W	16.0	8.1			

The disc wear tracks at the end of the tests are shown in Fig.12. On the uncoated cast iron disc, the presence of grey layers with a comparatively limited extension can be detected. They are made of iron oxides, proving that disc wear was mostly due to tribo-oxidation [34-36]. In case of A- and B-coated discs, darker areas are visible on the wear tracks. They are mainly made of fragments coming from the friction material (pin surface) transferred to the disc during the wear process, as confirmed by EDXS analysis. The extension of the friction layer on the disc surface was evaluated by means of image analysis, measuring the percentage of coverage. An example of this kind of analysis is shown by Fig. 12d, that refers to picture 12c. Image analysis data are all listed in Table 6.

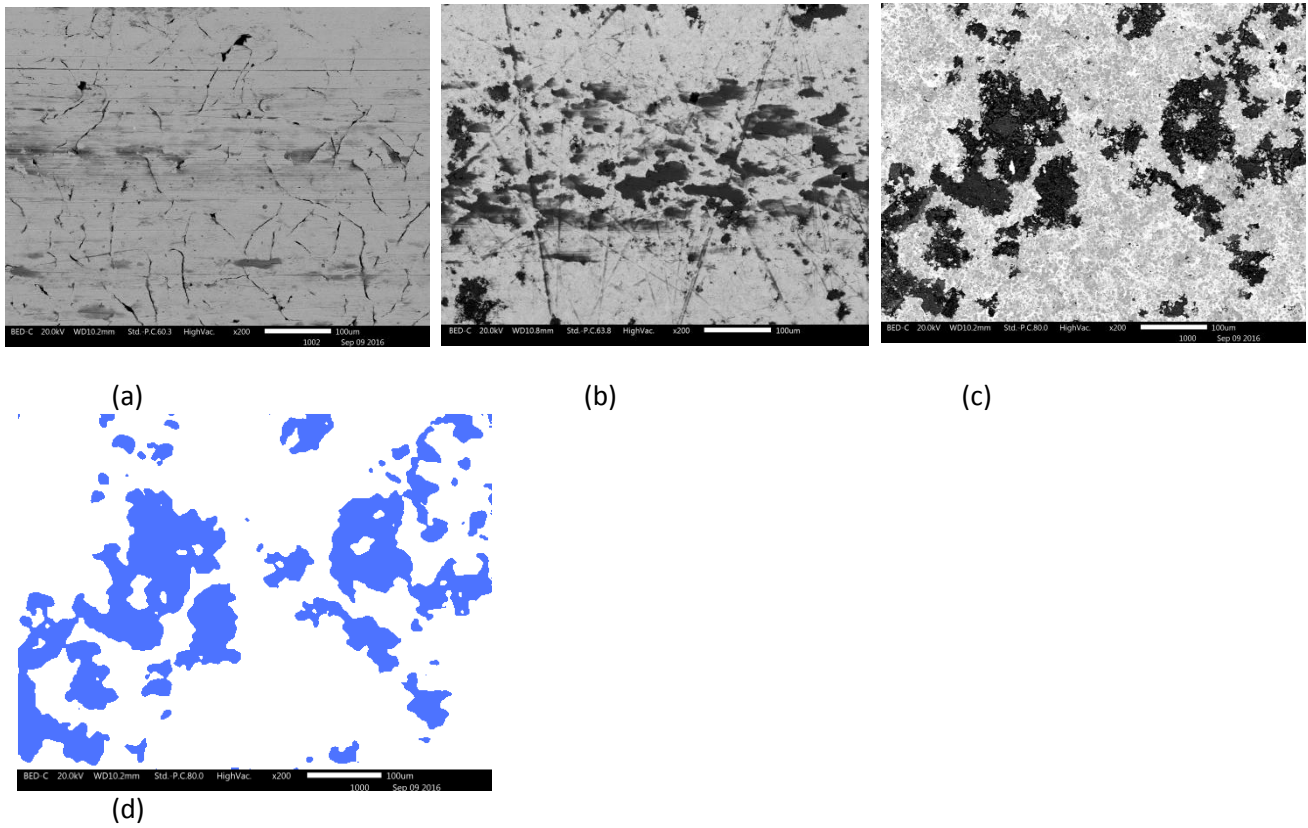


Fig.12. SEM micrographs of the wear tracks on the disc surface after PoD tests at room temperature. (a) Uncoated disc; (b) A Coating; (c) B Coating ; (d) example of output by the image analysis program used to measure transferred friction material on wear track (picture c).

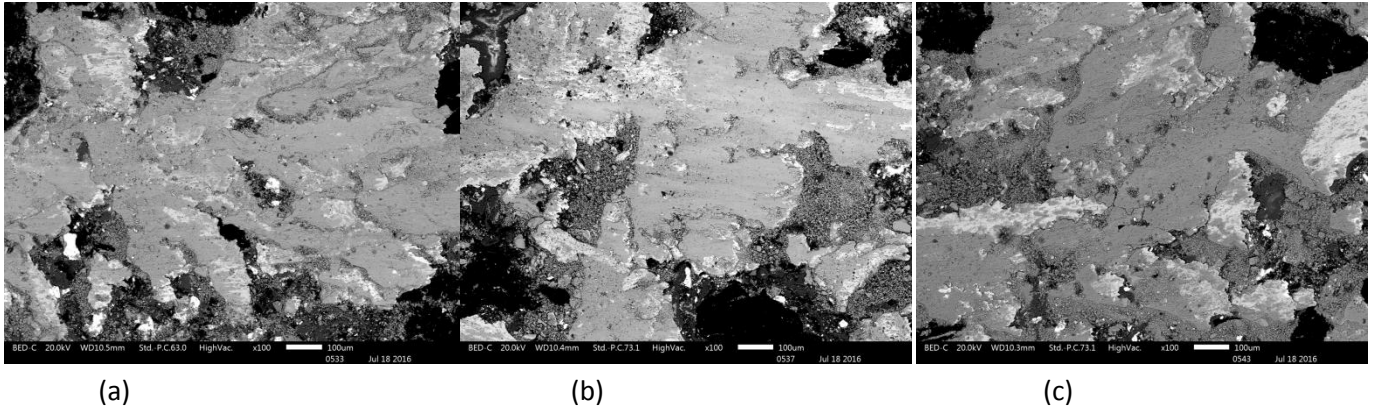
Table 6. Image analysis results on wear track of uncoated and coated discs indicating the % of coverage, as measured by image analysis.

	Fraction of worn surface covered with the friction layer (%)	
	RT	300°C
Uncoated	2.4	83.9
Coating A	15.1	30.1
Coating B	26.5	50

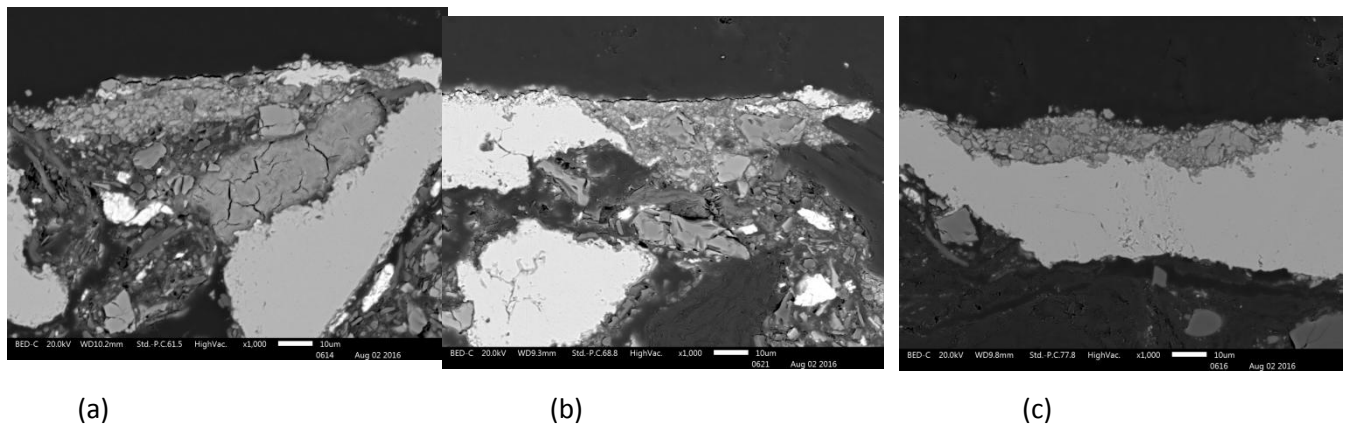
At the end of the PoD tests at 300°C, the friction layers are widely spread to cover a significant fraction of the pin surfaces, to a larger extent than after the test at room temperature. These features are displayed by the planar views in Fig.13. In particular, the secondary plateaus are made of larger fragments, as it can be observed in the cross sectional images of the friction layer (Fig.14). Some small cracks were also observed in the secondary plateaus, indicating that they reached a critical thickness and compaction degree and could break for longer test times. The thickness of these friction layers (up to 30 µm) is definitely larger than those observed after PoD tests at room temperature.

The EDXS analysis carried out on the secondary plateaus also show the presence of the pin material together with some transferred material from the coating (W and Co for the A-coated disc and Cr and Ni for the B-coated disc), as reported in Table 5. After PoD tests at 300°C, in all cases the composition of the friction layer tends to become quite similar to that of the friction material (compare with Table 2). For the coated discs, increasing the testing temperature up to 300°C is accompanied by a reduction of the

1 contribution of material from the disc (W and Co for coating A, Cr and Ni for coating B), because at this
2 temperature the main part of fragments is made of the friction material constituents.
3



19 Fig.13. SEM images of the planar views of the friction materials worn at 300°C against uncoated (a), A-
20 coated (b) and B-coated (c) discs respectively.
21



39 Fig.14. SEM images of the cross sections of friction materials worn at 300°C against uncoated (a), A-coated
40 (b) and B-coated (c) discs.
41

42
43
44
45 The wear tracks on the disc surface after the tests at 300°C were also examined. They are shown in
46 Fig.15. For the uncoated disc, the presence of the typical friction layer due to the tribo-oxidation of the cast
47 iron can be appreciated. In case of the coated discs, the friction layer is mainly resulting from the transfer
48 of the friction material from the pin. In Table 6 the results of the image analysis carried out to evaluate the
49 percentage of coverage of the disc worn surface by the friction layer are included. The wear track of the
50 uncoated disc is almost completely covered by oxides, while wear tracks of the discs with A and B coatings
51 are covered by compacted fragments and residues from the friction material. For them, the coverage
52 degree is double in comparison with the PoD tests at room temperature.
53
54
55
56
57
58
59
60
61
62
63
64
65

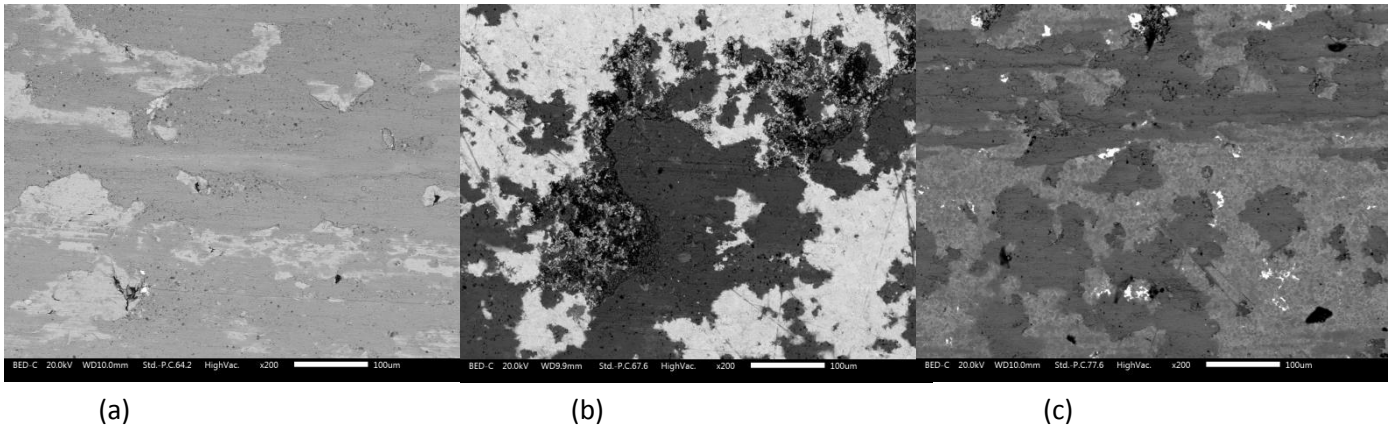


Fig.15. SEM micrographs of the wear tracks on the disc surface after PoD tests carried out at 300°C.

4 Discussion

The friction and wear behavior of low metallic friction materials sliding against pearlitic cast iron is generally determined by the characteristics of the friction layer that forms at the interface of the mating materials during sliding [19,20,37,38]. The layer on the surface of the friction material is typically formed by primary plateaus, made by quite hard and coarse ingredients of the friction material, and by secondary plateaus, resulting from the compaction of finer wear debris against the primary ones [19,20]. Such debris originates from the wear of the friction material and of the cast iron disc. The wear of the cast iron disc is typically tribo-oxidative in nature, involving the formation of Fe-oxide particles [20,38,39]. The friction layer that forms on the cast iron disc is typically obtained from the compaction of debris originating from both mating materials [40]. Friction is then determined by the adhesive and abrasive interactions between pin and disc. Wear is mainly determined by the disruption of the friction layers, and it is therefore governed by their compactness [5,19].

The tribological behavior of the friction materials under study, when sliding against the uncoated cast iron disc at room temperature, was coherent to the picture outlined above. In particular, the secondary plateaus on the friction material (the pin) were mainly made of compacted Fe-oxide particles. Therefore, the initial stage, characterized by a continuous increase in the friction coefficient (stage S1 in Figure 5a), can be attributed to the sliding period necessary to form well compacted secondary plateaus, thus leading to a steady-state friction coefficient. Such a steady-state was reached only close to the end of the test. Accordingly friction layers are characterized by the presence of debris spreading onto the primary plateaus and not always well compacted against them. The recorded pin wear was quite high and close to a severe wear regime [5,13]. This can be explained by considering that most of sliding occurred in the presence at the pin-disc interface of a low compacted friction layer with a high tendency to wear [19,20]. Additional tests carried out up to 7 hours of sliding, sufficient to stabilize an effective friction layer, revealed a decrease in the recorded wear rate down to $1.5 \cdot 10^{-14} \text{ m}^2/\text{N}$, i.e., a value quite typical of a mild wear regime [13].

In case of sliding against the coated discs at room temperature, the secondary plateaus on the friction material (the pin) are made by compaction of wear fragments originating from the friction material as well as from the coating, in agreement with a previous investigation [5]. In case of Coating A, the interaction in the contact regions was both adhesive and abrasive because of the high hardness of the coating asperities. The steady-state friction coefficient was thus slightly higher than the uncoated disc, because of the abrasive contribution. Coating B is softer than Coating A. As a consequence, a large transfer of coating particles onto to the pin surface, to form the secondary plateaus, was observed. This observation would indicate an easiest fragmentation of the coating. This favored a faster formation of the secondary plateaus, and therefore a reduction in the duration of the initial stage, S1 (Figure 6b). The steady-state friction coefficient was lower than for Coating A, because of the negligible contribution of the abrasive

1 interaction. The lower value of the steady-state friction coefficient with respect to the uncoated disc, can
2 be attributed to a lower adhesive interaction between the mating surfaces. Given the high number of
3 phases that are present in the friction layers, it is difficult to assign a leading role to any of them in
4 determining the friction behavior of the system. Nonetheless, the lower adhesive interaction can be
5 tentatively attributed to the lower amount of Fe-oxides in the secondary plateaus, which are expected to
6 promote the formation of quite high adhesive forces with the cast iron counterface and in particular with
7 the ferrous matrix [13]. With regard to the wear regime, it was mild in the case of the pin sliding against the
8 two coatings, whereas the coatings wear was negligible in both cases. The overall system wear with coated
9 discs was therefore lower than with uncoated disc.

10 As regards the sliding behavior of the uncoated disc at 300°C, the friction coefficient is rather
11 constant from the beginning of the test (Figure 8a). This means that a compact and dynamically stable
12 friction layer was formed quite soon. As a matter of fact, the high temperature greatly promotes the tribo-
13 oxidation of cast iron and, most importantly, the thermal degradation of the friction material with the
14 consequent formation of a wide and thick friction layer on the pin (Figures 13a and 14a). The
15 thermogravimetric analysis shown in Figure 4, revealed that degradation of the friction material should
16 start at 330°C approximately. However, it must be considered that during sliding the flash temperature at the
17 contacting asperities (the plateaus) was surely in excess of 300°C. Therefore, the observed thermal
18 phenomena are fully justified, even in view of the contribution to the degradation of the phenolic resin by
19 shear strain. The fact that the composition of the secondary plateaus on the pin surfaces is quite similar to
20 the composition of the friction material (compare Tables 2 and 5) means that the contribution of the pin
21 wear is quite high, and it overwhelms that due to the transfer of Fe-oxide from the disc counterface. The
22 tribo-oxidation of the cast iron disc was however quite pronounced, as revealed by the observation of the
23 worn surfaces (Figure 15a). Together with the well known fading effects connected with the thermal
24 degradation of the friction material [21-23], this effect contributed to decreasing the steady-state friction
25 coefficient with respect to the value measured at room temperature, because of the well known, albeit
26 limited, solid lubricant effect exerted by the Fe-oxides [31,41]. The wear of the friction material (the pin)
27 was quite high because of the above-mentioned thermal softening effects. It is similar to the value
28 recorded at room temperature, because at room temperature wear was really high, as explained above.
29 The very large transfer of material onto the disc surface (see Table 6) promoted by the thermal softening,
30 rendered impossible the record of the disc wear.

31 In case of Coating A, tested at 300°C, the friction coefficient initially increased to approximately
32 0.60 and then decreased to approximately 0.55 (Figure 9a). Such initial increase in the friction coefficient
33 can be attributed to the abrasive interaction of the hard asperities, whose intensity decreased with the
34 rapid formation of a widely spread and thick friction layer. The steady-state friction coefficient was then
35 lower than that recorded at room temperature, because of the above-mentioned fading effects, due to the
36 thermal degradation of the friction material. Thermal softening was also responsible for the increase in the
37 wear rate of the pin (Table 4). The lower hardness of Coating B induced a lower abrasive interaction of the
38 asperities and therefore a steady state was reached almost from the beginning of the test. Also in this case,
39 the thermal degradation effects of the friction material induced a decrease in the friction coefficient and a
40 considerable increase in the wear rate of the friction material with respect to the values recorded at room
41 temperature.

42 Eventually, it must be noted that also for the tests carried out at 300°C the wear of the coatings
43 was negligible and in agreement with the results obtained at room temperature. As seen in the
44 Introduction, the thermal degradation of the coatings, with softening or oxidative effects, can be triggered
45 at temperatures well in excess of 400-600°C that were not attained during sliding in the present
46 investigation.

57 **5 Conclusions**

58
59 The wear behavior of a commercial friction material dry sliding against two types of HVOF coatings
60 was investigated at room temperature as well as at 300°C using a PoD apparatus. The main findings can
61 be summarized as follows:
62
63
64
65

- At room temperature and in the selected testing conditions, the friction material sliding against the uncoated disc requires a comparatively long time to reach a steady-state, featuring a constant friction coefficient. As a consequence, the friction layer is characterized by the presence of poorly compacted secondary plateaus, and the wear rate is quite high.
- In case of sliding against the two coatings, a constant friction coefficient is reached sooner, in particular for Coating B that possess a lower hardness than Coating A. In both cases, the wear of the friction material (the pin) is mild and the wear of the coated discs is negligible.
- The thermogravimetric analysis shows that the friction material undergoes a thermal softening starting from 330°C due to the decomposition of the phenolic binder. During sliding at 300°C (that is the temperature of the disc), the temperature in the contact regions (the plateaus) is definitely higher than 300°C, thus justifying the thermal softening effects observed during sliding.
- At 300°C, thermal softening induced in all cases the formation of a wide and thick friction layer from almost the beginning of the tests, and therefore the friction coefficient was almost constant during the tests (with the exception of Coating A that showed a small increase in the friction coefficient at the beginning of the test).
- As expected, the wear rates of the friction materials were quite high irrespective of the counterface material. It was not possible to measure any wear from the uncoated disc because of the large transfer induced by thermal softening.
- The wear rates of the coated discs were negligible also at 300°C, in agreement with the fact that the contact temperature were too low to induce any large-scale damage of the HVOF coating, that should start at temperatures above 400-500°C (as shown by the literature).

Ongoing research is focusing on the role of disc temperatures even above 300°C in order to establish the role of possible softening of oxidative damages of the coatings and reveal possible differences in the sliding behavior of the two coatings under study, even if such high temperature are not quite common in practical situations. The low system wear is of course promising with regard to braking applications and the possible reduction of PM emissions in the environment. Specific dynamometer and bench tests need to be carried out in order to confirm the results obtained so far and for evaluating the performance of real braking systems.

Acknowledgment

The research leading to these results received funding from the European Union's Horizon 2020 research and innovation programme under grant agreement No. 636592 (LOWBRASYS project).

References

- [1] J. Wahlstrom, L. Olander, U. Olofsson, A pin-on-disc study focusing on how different load levels affect the concentration and size distribution of airborne wear particles from the disc brake materials, *Tribol. Lett.* 46 (2012) 195–204.
- [2] P. Sanders, N. Xu, T.M. Dalka, M.M. Maricq, Airborne brake wear debris: size distributions, Composition, and a comparison of dynamometer and vehicle tests, *Environ. Sci. Technol.* 37 (2003) 4060–4069.
- [3] G. Straffelini, R. Ciudin, A. Ciotti, S. Gialanella, Present knowledge and perspectives on the role of copper in brake materials and related environmental issues: a critical assessment, *Environ. Pollut.* 207 (2015) 211–219.
- [4] J. Wahlstrom, A. Södeberg, L. Olander, A. Jansson, U. Olofsson, A pin-on-disc simulation of airborne wear particles from disc brakes, *Wear* 268 (2010) 763-769.
- [5] M. Federici, C. Menapace, A. Moscatelli, S. Gialanella, G. Straffelini, Effect of roughness on the wear behavior of HVOF coatings dry sliding against friction material, *Wear* 368-369 (2016) 326-334.
- [6] J.K.N. Murthy, B. Venkataraman, Abrasive wear behavior of WC-CoCr and Cr₃C₂-20(NiCr) deposited by HVOF and detonation spray processes, *Surf. Coat. Technol.* 200 (2006) 2642-2652.
- [7] J.R. Davis(Ed.), *Handbook of Thermal Spray Technology*, ASM International, Materials Park, OH, USA, 2004.
- [8] Q. Wang, Z. Chen, Z. Ding, Performance of abrasive wear of WC-12Co coatings sprayed by HVOF, *Tribol. Int.* 42 (7) (2009) 1046-1051
- [9] Y. Ishikawa, S. Kuroda, J. Kawakita, Y. Sakamoto, M. Takaya, Sliding wear properties of HVOF sprayed WC-20%Cr₃C₂-7%Ni cermet coatings, *Surf. Coat. Technol.* 201 (2007) 4718-4727,
- [10] W. Zhang, L. Liu, M. Zhang, G. Huang, J. Liang, X. Li, L. Zhang, Comparison between WC-10Co-4Cr and Cr₃C₂-25NiCr coatings sprayed on H13 steel by HVOF, *Trans. Nonferrous Met. Soc. China* 25 (2015) 3700-3707,
- [11] A. Siao Ming Ang, H. Howse, S.A. Wade, C.C. Berndt, Development of processing windows for HVOF carbide-based coatings, *J. Therm. Spray Techn.* 22 (2013) 280-289
- [12] G.M. La Vecchia, F. Mor, G. Straffelini, D. Doni, Microstructure and sliding wear behavior of thermal spray carbide coatings, *Int. J. Powder Metall.* 35 (1999) 37-46.
- [13] G. Straffelini, *Friction and Wear, Methodologies for Design and Control*, Springer International Publishing, Switzerland, 2015.
- [14] H.L. De Villiers Lovelock, Powder/processing/structure relationships in WC–Co thermal spray coatings: a review of the published literature, *J. Therm. Spray Techn.* 7 (1998) 357–373.
- [15] M.R. Dorfman, B.A. Kushner, J. Nerz, A.J. Rotolico, A technical assessment of high velocity oxygen-fuel versus high energy plasma tungsten carbide–cobalt coatings for wear resistance, in: *Proceedings of the 12th International Thermal Spray Conference*, London, 1989, pp.291–302.
- [16] H. Wang, X. Wang, X. Song, X. Liu, X. Liu, Sliding wear behavior of nanostructured WC-Co-Cr coatings, *Appl. Surf. Sci.* 355 (2015) 453-460.
- [17] G. Bolelli, L.M. Berger, M. Bonetti, L. Lusvarghi, Comparative study of the dry sliding wear behavior of HVOF-sprayed WC-(W,Cr)₂C-Ni and WC-CoCr hardmetal coatings, *Wear* 309 (2014) 96-111.
- [18] M. Watremez, J.P. Bricout, B. Marguet, J. Oudin, Friction, temperature, and wear analysis for ceramic coated brake disks, *J. Tribol.* 118 (1996) 457-465.
- [19] M. Eriksson, F. Bergman, F. Jacobson, On the nature of tribological contact in automotive brakes, *Wear* 252 (2002) 26-36.
- [20] M. Eriksson, F. Jacobson, Tribological surfaces of organic brake pads, *Tribol. Int.* 33 (2000) 817-827.
- [21] P.C. Verma, R. Ciudin, A. Bonfanti, P. Aswath, G. Straffelini, S. Gialanella, Role of the friction layer in the high-temperature pin-on-disc study of a brake material, *Wear* 346-347 (2016) 56-65.
- [22] S. Ramousse, J.W. Hoj, O.T. Sørensen, Thermal characterization of brake pads, *J. Therm. Anal. Calorim.* 64 (2001) 933–943.
- [23] K. Bode, G.P. Ostermeyer, A comprehensive approach for the simulation of heat and heat-induced phenomena in friction materials, *Wear* 311 (2014) 47–56.

- 1 [24] J. Kukutschová, P. Moravec, V. Tomásek, V. Matejka, J. Smolík, J. Schwarz, J. Seidlerová, K. Safárová, P.
2 Filip, On airborne nano/micro-sized wear particles released from low-metallic automotive brakes, *Environ.*
3 *Pollut.* 159 (2011) 998-1006.
- 4 [25] M.A. Zavareth, A.A.D.M. Sarhan, B.B.A. Razak, W.J. Basirun, The tribological and electrochemical
5 behavior of HVOF-spayed Cr₃C₂-NiCr ceramic coating on carbon steel, *Ceram. Int.* 41 (2015) 5387-5396.
- 6 [26] A. Lekatou, D. Sioulas, A.E. Karantzalis, D. Grimanelis, A comparative study on the microstructure and
7 surface property evaluation of coatings produced from nanostructured and conventional WC-Co powders
8 HVOF-sprayed on Al7075, *Surf. Coat. Technol.* 276 (2015) 539-556.
- 9 [27] G. Skandan, R. Yao, B.H. Kear, Y.Qiao, L. Liu, T.E. Fischer, *Scripta Materialia* 44 (2001) 1699.
- 10 [28] C. Verdon, A. Karimi, J.-L. Martin, A study of high velocity oxy-fuel thermally sprayed tungsten
11 carbide based coatings. Part 1: Microstructures, *Mat. Sci. Eng. A246* (1998) 11-24.
- 12 [29] L. Lutterotti, Total pattern fitting for the combined size-strain-stress-texture determination in thin film
13 diffraction. *Nucl Inst Methods Phys Res* 2010; B268:334-40.
- 14 [30] P.H. Shipway, D.G. McCartney, T. Sudaprasert, Sliding wear behaviour of conventional and
15 nanostructured HVOF sprayed WC-Co coatings, *Wear* 259 (2005) 820-827.
- 16 [31] P.C. Verma, L. Menapace, A. Bonfanti, R. Ciudin, S. Gialanella, G. Straffelini, Braking pad-disc system:
17 wear mechanisms and formation of wear fragments, *Wear* 322-323 (2015) 251-258.
- 18 [32] P.H. Shipway, D.G. McCartney, T. Sudaprasert, Sliding wear behavior of conventional and
19 nanostructured HVOF sprayed WC-Co coatings, *Wear* 259 (2005) 820-827.
- 20 [33] J. Pirso, S. Letunovitis, M. Viljus, Friction and wear behavior of cemented carbides, *Wear* 257 (2004)
21 257-265.
- 22 [34] G. Straffelini, M. Pellizzari, L. Maines, Effect of sliding speed and contact pressure on the oxidative
23 wear of austempered ductile iron, *Wear* 270 (2011) 714-719.
- 24 [35] I.M. Hutchings, *Friction and Wear of Engineering Materials*, Edward Arnold, London, 1992.
- 25 [36] G. Straffelini, A. Molinari, Mild sliding wear of Fe-0.2%C, Ti-6%Al and Al-7072: a comparative study,
26 *Tribol. Lett.* 41 (2011) 227-238.
- 27 [37] G. Straffelini, L. Maines, The relationship between wear of semimetallic friction materials and pearlitic
28 cast iron in dry sliding, *Wear* 307 (2013) 75-80.
- 29 [38] G. Straffelini, P.C. Verma, I. Metinoz, R. Ciudin, G. Perricone, S. Gialanella, Wear behavior of a low
30 metallic friction material dry sliding against a cast iron disc: Role of the heat-treatment of the disc, *Wear*
31 348-349 (2016) 10-16.
- 32 [39] R. Hinrichs, M.A.Z. Vasconcellos, W. Österle, C. Prietzel, A TEM snapshot of magnetite formation in
33 brakes: The role of the disc's cast iron graphite lamellae in third body formation, *Wear* 270 (2011) 365-370.
- 34 [40] W. Österle, I. Urban, Third body formation on brake pads and rotors, *Tribol. Int.* 39 (2006) 401-408.
- 35 [41] H. Kato, Severe-mild wear transition by supply of oxide particles on sliding surface, *Wear* 255 (2003)
36 426-429.
- 37
38
39
40
41
42
43
44
45
46
47
48
49
50
51
52
53
54
55
56
57
58
59
60
61
62
63
64
65

Figure Captions

1
2
3 Fig.1. SEM micrographs showing the cross section of the as-sprayed coatings A (a) and B (b).
4

5 Fig.2. XRD spectra of coatings A (a) and B (b).
6

7
8 Fig.3. SEM micrograph of the surface of the friction material, with the indication of some of the main
9 components
10

11 Fig.4. TG and DTG curves of friction material.
12

13
14 Fig.5. Evolution of the friction coefficient μ as a function of the wear test time (a) and contact temperature
15 of pin measured by thermocouple at 4 mm (T1) and 6 mm (T2) from the disc surface during the test against
16 the uncoated disc at room temperature (b).
17

18
19 Fig.6. Evolution of the friction coefficient μ during wear tests carried out at room temperature. (a) results
20 fore the A (a) and B (b) coated disc.
21

22 Fig.7. Wear track profile present on the disc surface after room temperature PoD tests. (a) Uncoated disc;
23 (b) Coating A; (c) Coating B.
24

25
26 Fig. 8. Evolution of the friction coefficient μ (a) and of the pin temperature (b), during wear test against
27 conducted with the uncoated disc at 300°C.
28

29
30 Fig.9. Evolution of the friction coefficient and of the pin temperature during PoD tests conducted on the
31 two coating systems considered in the present study: Coating A: (a), (b); coating B: (c), (d).
32

33 Fig.10. SEM micrographs of the planar views of friction materials PoD tested at room temperature, against
34 uncoated (a), A-coated (b) and B-coated (c) discs.
35

36
37 Fig.11. Cross sectional SEM images of the worn surface of the friction materials PoD tested at room
38 temperature against uncoated (a), A-coated (b) and B-coated (c) discs.
39

40 Fig.12. SEM micrographs of the wear tracks on the disc surface after PoD tests at room temperature. (a)
41 Uncoated disc; (b) A Coating; (c) B Coating ; (d) example of output by the image analysis program used to
42 measure transferred friction material on wear track (picture c).
43

44
45 Fig.13. SEM images of the planar views of the friction materials worn at 300°C against uncoated (a), A-
46 coated (b) and B-coated (c) discs respectively.
47

48
49 Fig.14. SEM images of the cross sections of friction materials worn at 300°C against uncoated (a), A-coated
50 (b) and B-coated (c) discs.
51

52 Fig.15. SEM micrographs of the wear tracks on the disc surface after PoD tests carried out at 300°C.
53
54
55
56
57
58
59
60
61
62
63
64
65